

Supplementary Information

Precise and Selective Macroscopic Assembly of Dual Lock-and-Key Structured Hydrogel

Eunseok Heo^a, Wooseop Hwang^b, Hye Been Koo^a, Steve Park^a, Do-Nyun Kim^c, Ho-Young Kim^c, YongJoo Kim^b, and Jae-Byum Chang^{*ad}

^aDepartment of Materials Science and Engineering, Korea Advanced Institute of Science and Technology (KAIST), Daejeon, 34141, Republic of Korea

^bDepartment of Materials Science and Engineering, Kookmin University, Seoul 02707, Republic of Korea

^cDepartment of Mechanical Engineering, Seoul National University, Seoul 08826, Republic of Korea

^dDepartment of Biological Sciences, Korea Advanced Institute of Science and Technology (KAIST), Daejeon 34141, Republic of Korea

**E-mail: jbchang03@kaist.ac.kr*

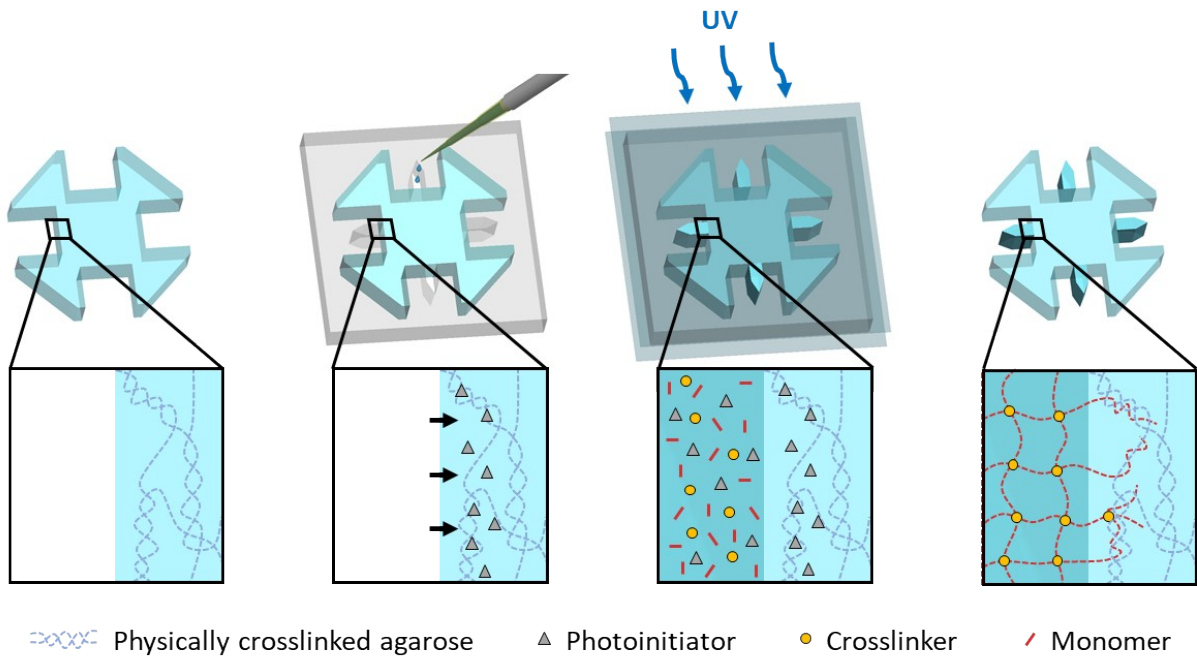


Fig. S1 Schematic illustration of the overall fabrication process for the chemically heterogeneous hydrogel building blocks.

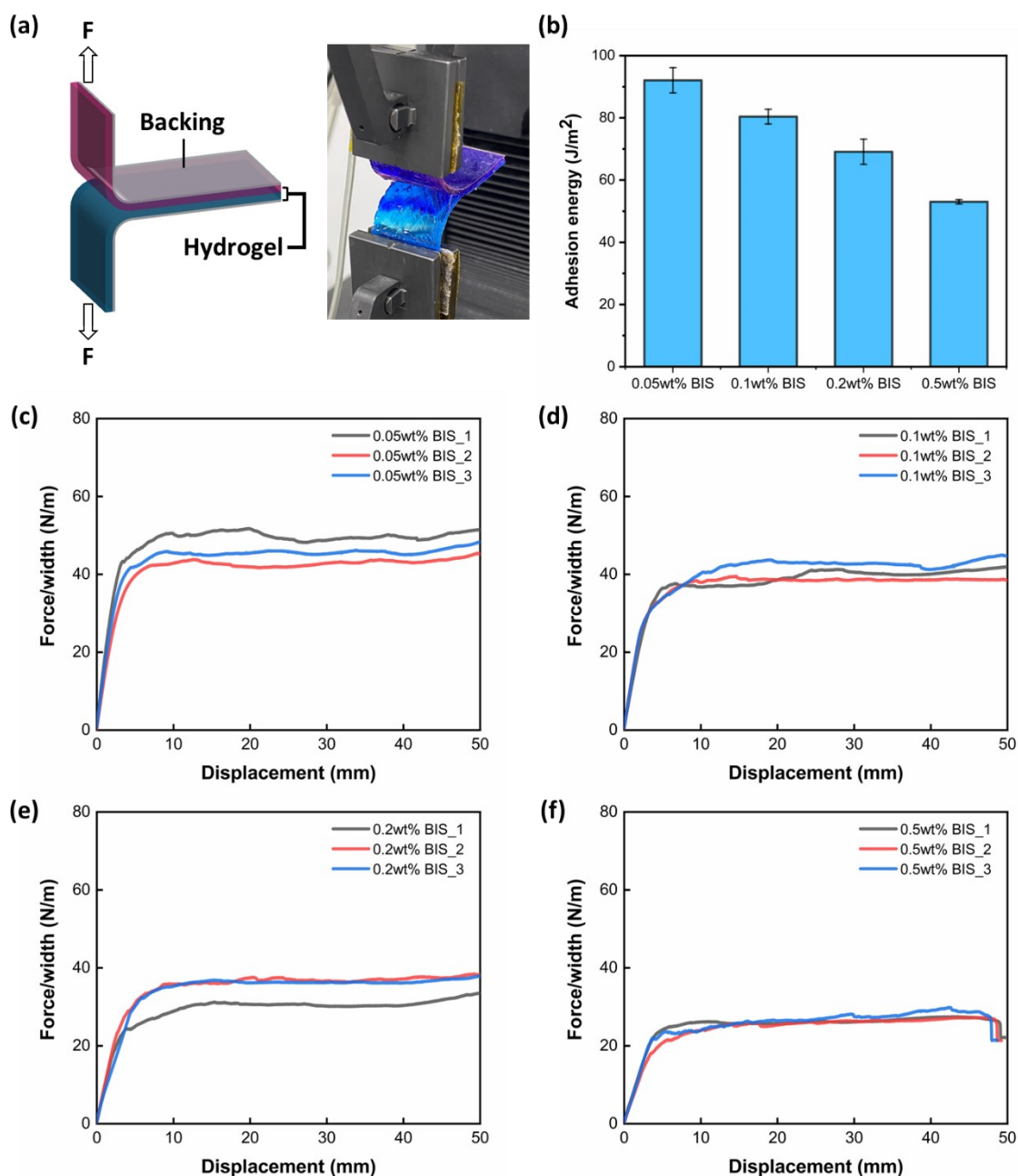


Fig. S2 (a) Schematic illustration and experimental image of a 180°-peeling test. (b) Adhesion energies between the oppositely charged hydrogels, varying the crosslinker concentrations. Representative force/width-displacement curved of the 180°-peeling test with crosslinker concentrations of (c) 0.05 wt%, (d) 0.1 wt%, (e) 0.2 wt%, and (f) 0.5 wt%.

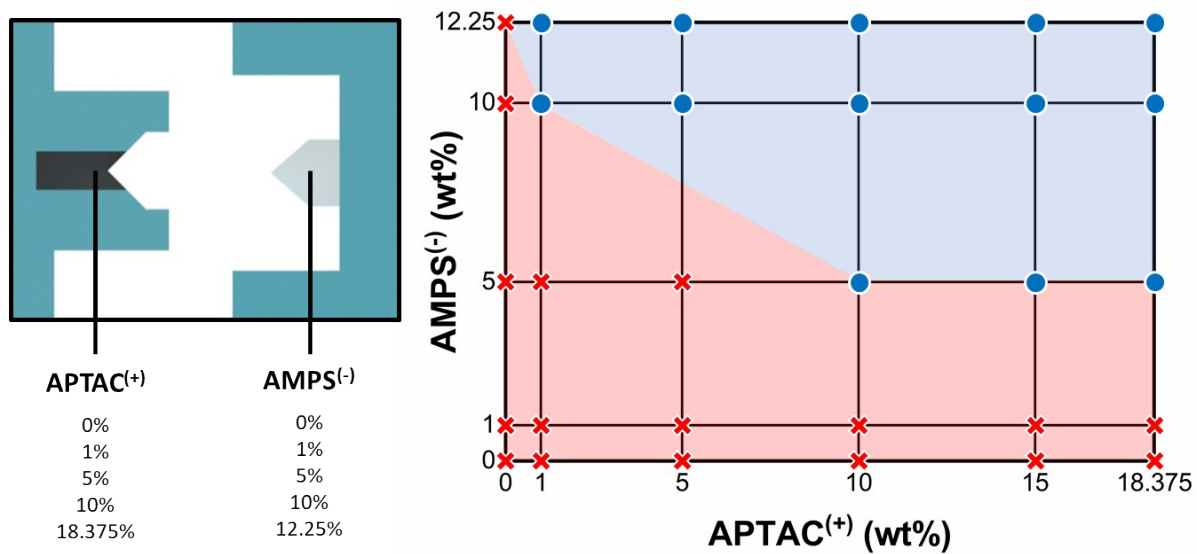
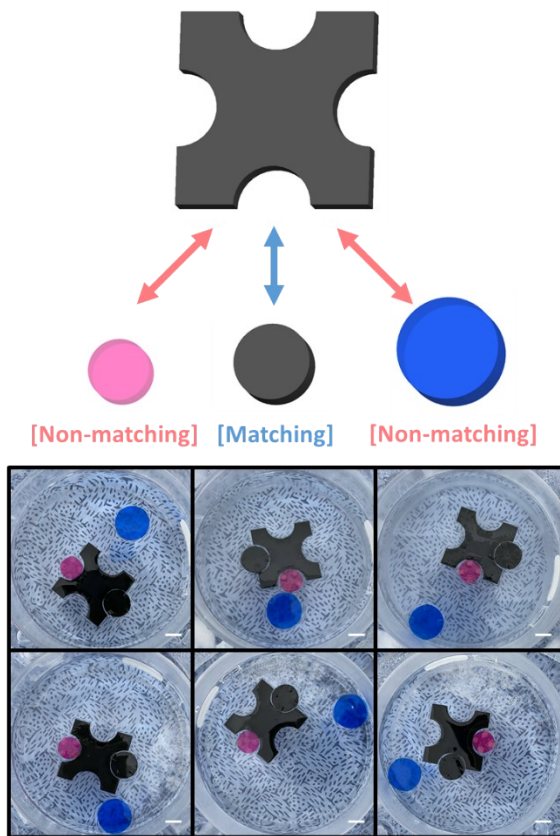


Fig. S3 Assembly stability test between charged hydrogels by varying the concentration of positively and negatively charged monomers.

(a) Single lock-and-key



(b) Dual lock-and-key

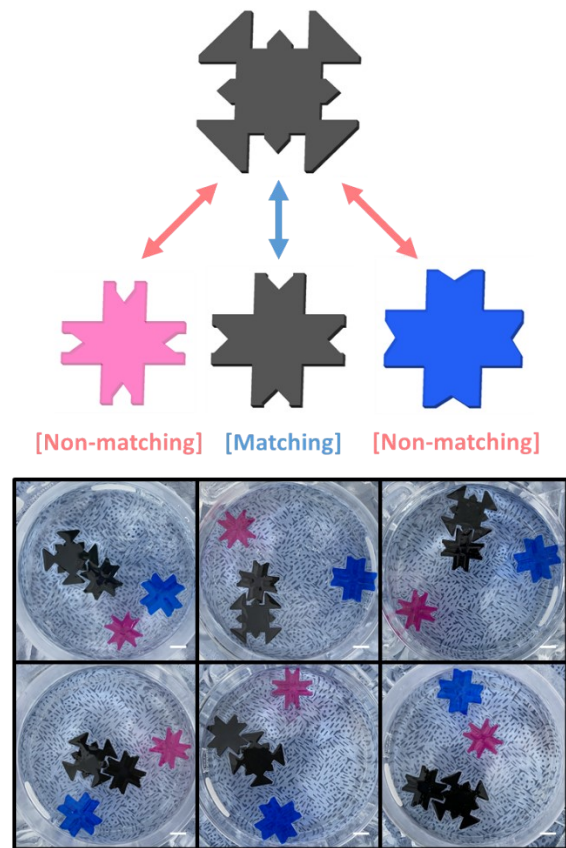
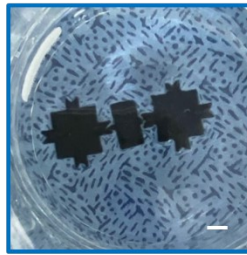
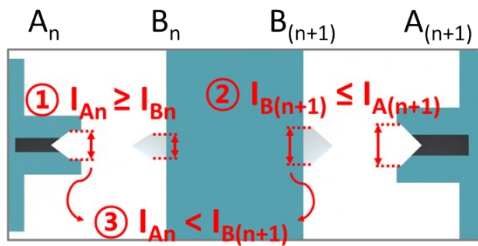
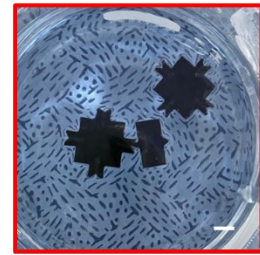


Fig. S4 Design schematics and experimental images displaying (a) assembly using the single lock-and-key structures, and (b) assembly using the dual lock-and-key structures. Scale bars: 1 cm.

(a) Inner lock-and-key-controlled assembly

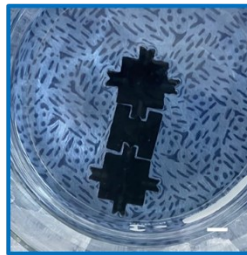
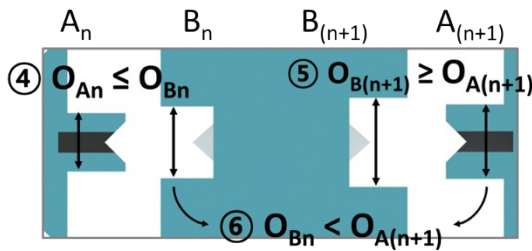


Matching pairs: 56%
(5/9)

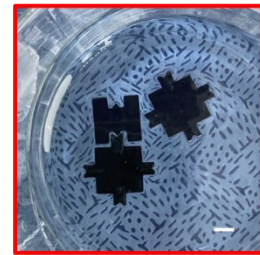


Non-matching pairs: 44%
(4/9)

(b) Outer lock-and-key-controlled assembly

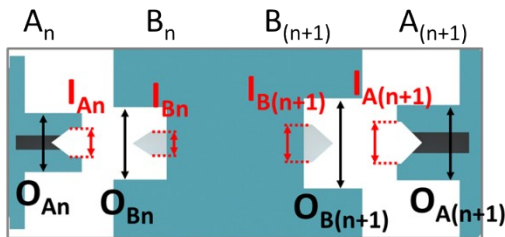


Matching pairs: 78%
(7/9)

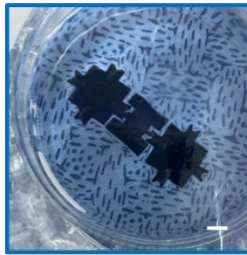


Non-matching pairs: 22%
(2/9)

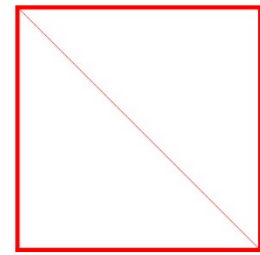
(c) Dual lock-and-key-controlled assembly



[Satisfies both ①-③, ④-⑥]



Matching pairs: 100%
(9/9)



Non-matching pairs: 0%
(0/9)

Fig. S5 Design schematics and assembly yields of the building blocks to assess the accuracy of the dual lock-and-key-assisted selective assembly when controlled by (c) the inner lock-and-key only, (d) the outer lock-and-key only, and (e) the dual lock-and-key. Scale bars: 1 cm.

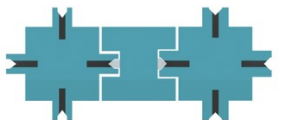
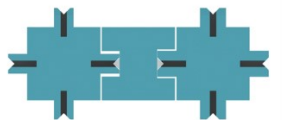
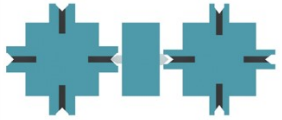
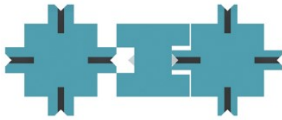
Inner lock-and-key only		Outer lock-and-key only		Dual lock-and-key	
Matching pair	$A_n - [B_n - B_{n+1}] - A_{n+1}$	Matching pair	$A_n - [B_n - B_{n+1}] - A_{n+1}$	Matching pair	$A_n - [B_n - B_{n+1}] - A_{n+1}$
					
Non-matching pair	$A_{n+1} - [B_n - B_{n+1}] - X$	Non-matching pair	$X - [B_n - B_{n+1}] - A_n$	Non-matching pair	-
					

Fig. S6 Schematic illustrations of the possible matches and non-matches between the hydrogel building blocks, controlled by the two lock-and-keys depicted in Fig. 2c-e.

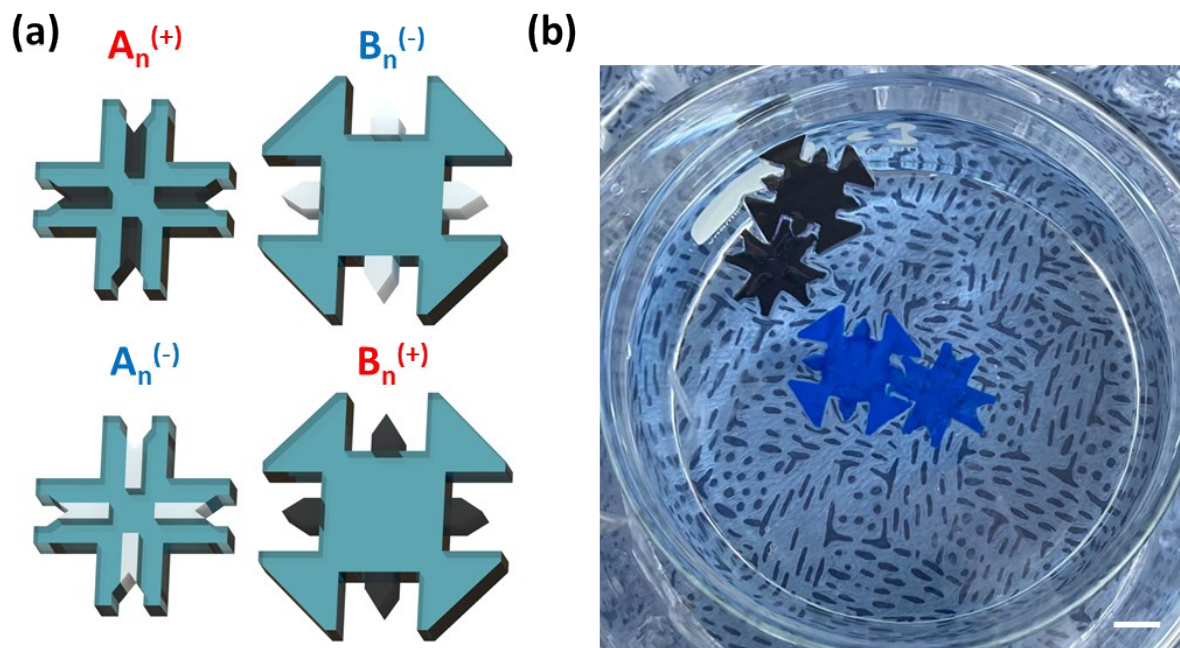


Fig. S7 (a) Schematic illustrations of two hydrogel building blocks with identical designs but different charge arrays. (b) Experimental image demonstrating selective assembly only between oppositely charged pairs. Scale bars: 1 cm.

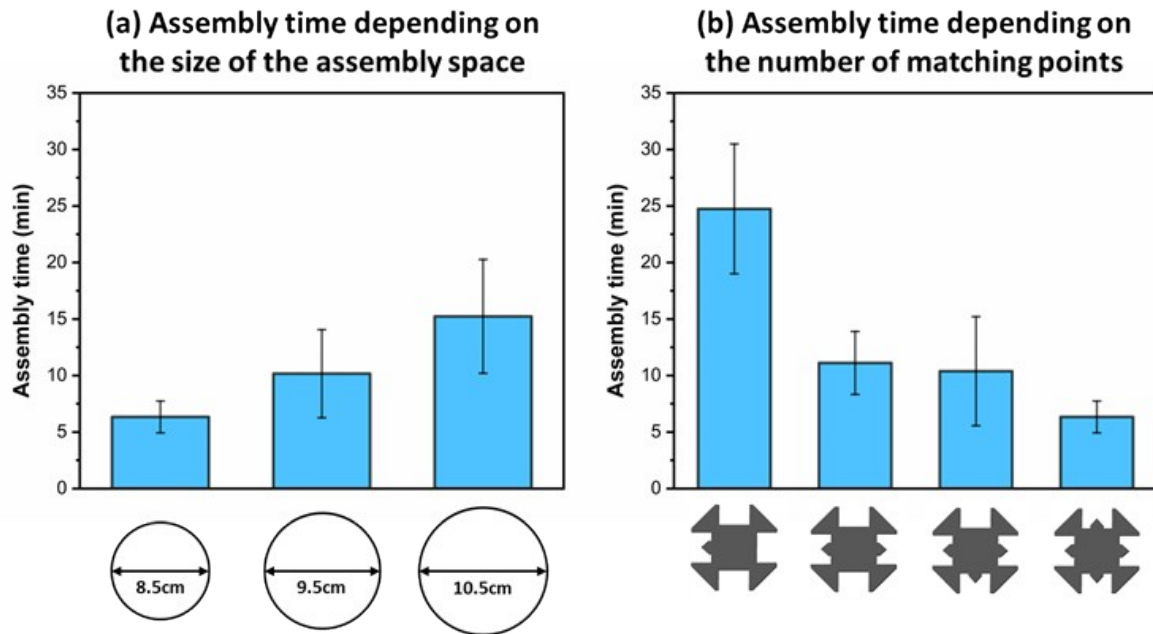


Fig. S8 Graphs depicting the time consumed for assembly using the dual lock-and-key structure depending on (a) the size of the assembly space while maintaining four matching points ($n=5$ for each case), and (b) the number of matching points in a single building block with an 8.5 cm dish size ($n=5$ for each case). The size of the hydrogel building blocks was 23.8 mm in width, while the size of the corresponding matching pair was 19.8 mm.

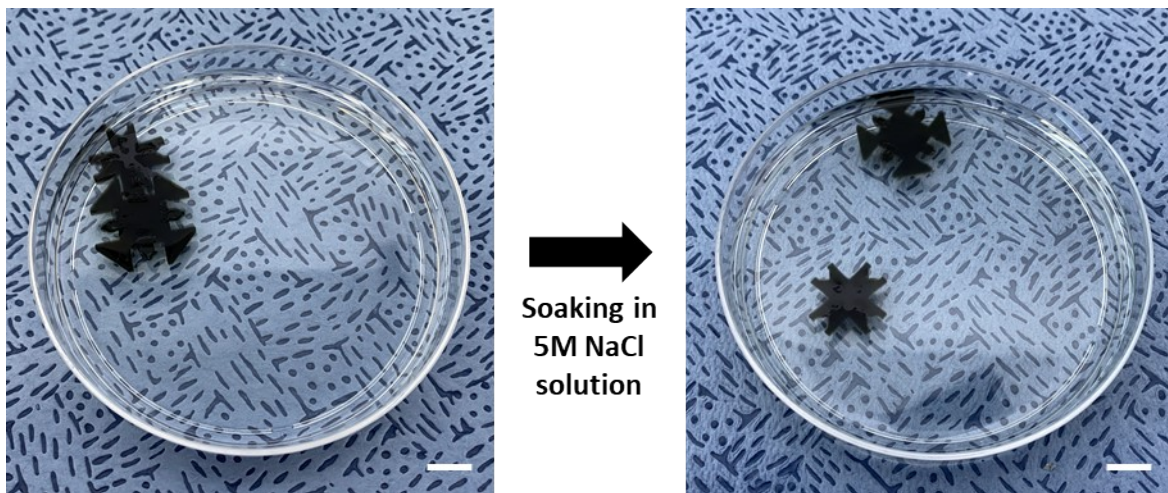


Fig. S9 Experimental images of demand detachment of the assembled hydrogel building blocks under salt conditions. Scale bars: 1 cm.

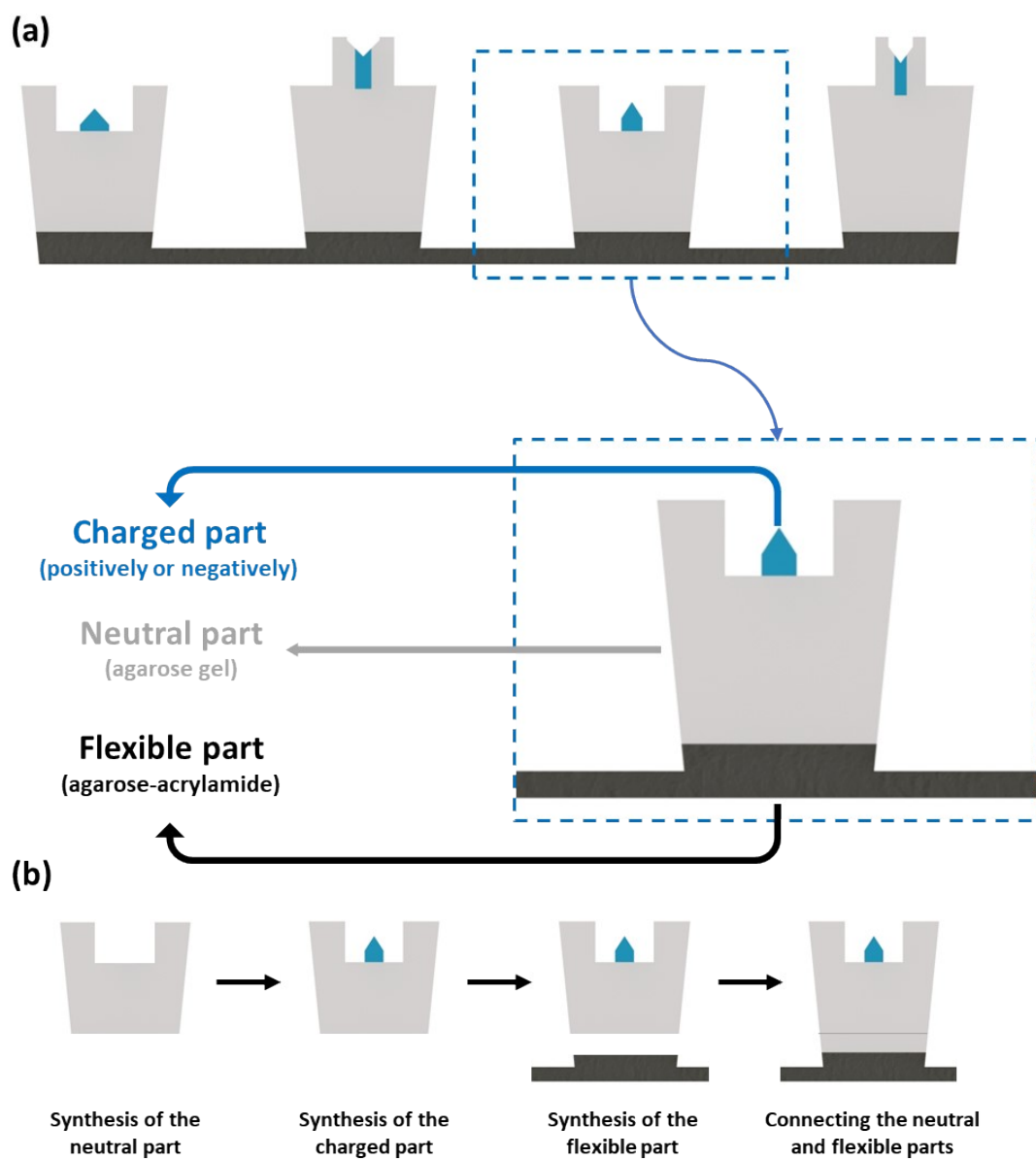


Fig. S10 (a) Schematic illustrations of DNA-mimicking double-stranded structures, consisting of three components: a charged part, a neutral part, and a flexible part. (b) Synthesis procedure for DNA-mimicking structures.

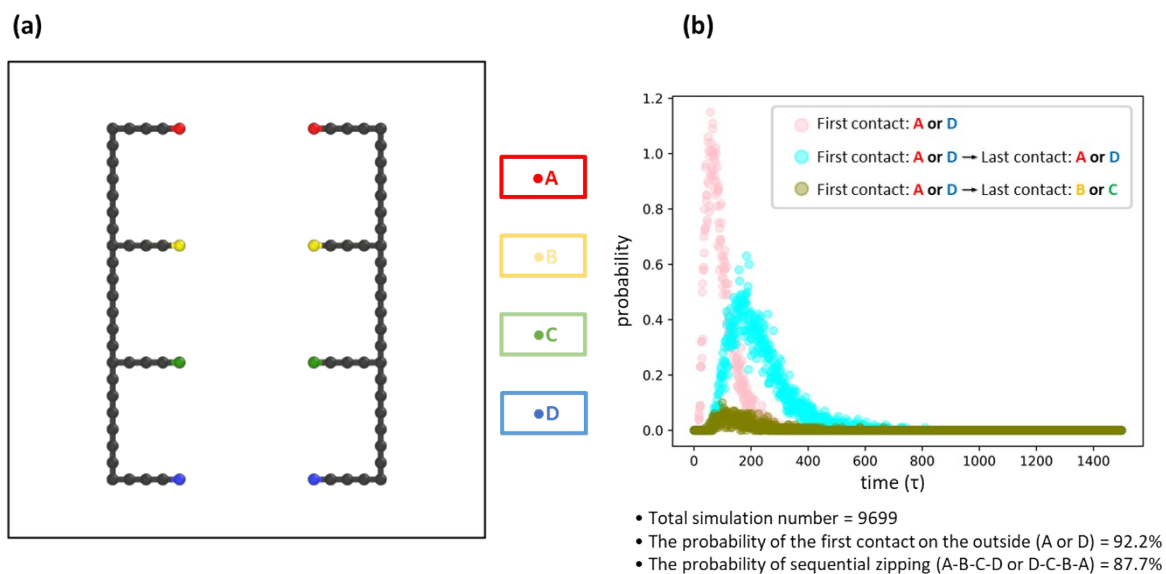


Fig. S11 (a) Designed model of a DNA-mimicking structure for molecular dynamics simulation. (b) Graph depicting the probability of the assembly spot for the first and last contact.

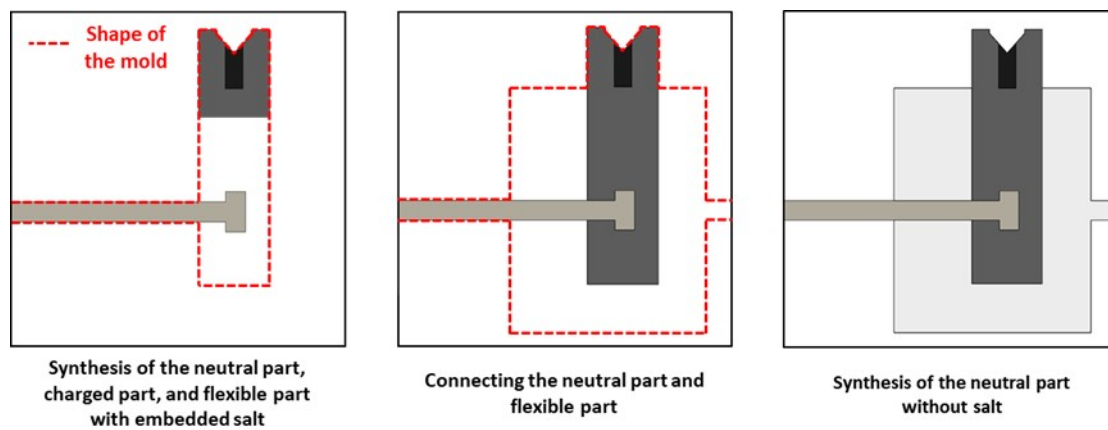


Fig. S12 Synthesis procedure for the hydrogel-based logic gate.

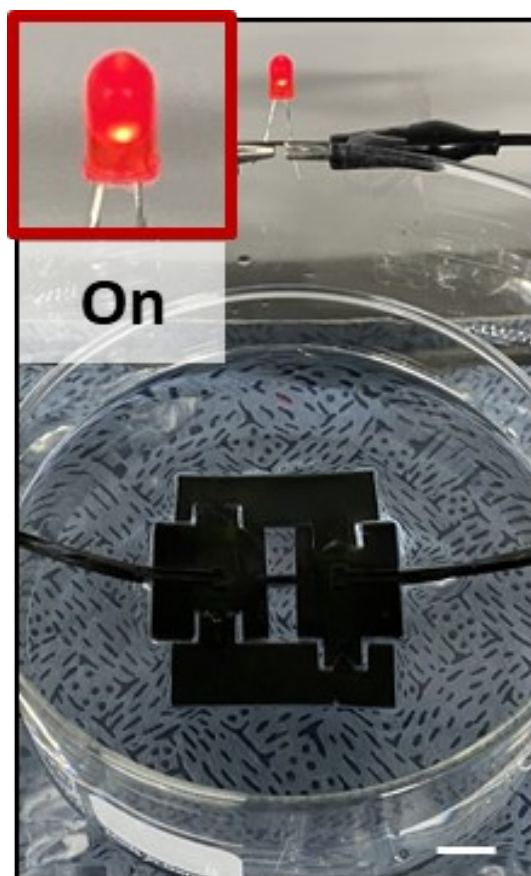


Fig. S13 Experimental image showing the connection of the two complementary building blocks to the main part in the OR logic gate.